EurJOC European Journal of Organic Chemistry

FULL PAPER

DOI: 10.1002/ejoc.201301085

Tuning the Photophysical Properties of 2-Quinolinone-Based Donor–Acceptor Molecules through *N*- versus *O*-Alkylation: Insights from Experimental and Theoretical Investigations

Ganesan Paramaguru,[a] Rajadurai Vijay Solomon,[a] Sivanadanam Jagadeeswari,[a] Ponnambalam Venuvanalingam,*[a] and Rajalingam Renganathan*[a]

Keywords: Donor-acceptor systems / Tautomerism / Fluorescence spectroscopy / Density functional calculations / Sensors

A series of 2-quinolinone-based molecular systems with three different acceptor groups and N/*O*-alkylated quinolinone compounds have been synthesised in an attempt to understand their optical properties. All the compounds were characterised by ^{1}H NMR, ^{13}C NMR and mass analysis. Absorption measurements revealed that charge-transfer transition was observed by introducing electron-withdrawing acceptor groups. Alkylation of 2-quinolinone at the O-position thwarts the charge-transfer transitions, whereas *N*-alkylation retains the charge-transfer property. The presence of resonance zwitterionic forms in the unalkylated and *N*-alkylated quinolinone compounds play an important role in charge-transfer transition. The effects of solvents on the absorption and emission properties of these compounds were probed through Lippert Mataga and $E_T(30)$ correlation. The Stokes shifts of *O*-alkylated compounds were larger than those of the unalkylated and *N*-alkylated quinolinone compounds. The observed higher quantum yield and Stokes shift for these compounds will make them ideal fluorescent probes. Incorporation of acceptor groups and alkylation in the quinolinone moiety alters their energy levels. Good thermal stability was observed for both unalkylated and alkylated quinolinone compounds. The trends observed in the photophysical and electrochemical properties were supported by theoretical studies. The observed tunable optical properties, which were achieved through simple *N*- vs. *O*-alkylation, results in large Stokes shifts and thermal stability, which means that the 2-quinolinone-based molecular systems are expected to emerge as potential candidates for photovoltaic and biological applications.

Introduction

Donor–Acceptor molecular systems possess intramolecular charge transfer (CT) properties, which is one of the key parameters for their potential applications in various fields such as organic photovoltaics, organic light-emitting diodes, nonlinear optical (NLO) materials, and biological sensors.[1] The CT properties of these systems can be easily tuned by linking suitable donor and acceptor moieties. Over the years, donor fragments such as pyrene, perylene, triphenylamine, carbazole, coumarin, phenothiazine, and indoline, and acceptor moieties such as cyano, nitrophenyl acrylonitrile, carboxylate, and rhodanine substituents have been successfully employed as donor–acceptor systems for various applications.[2] Molecular systems that show large Stokes shift are widely utilized as fluorescent probes for biological applications, UV photostabilisers, laser dyes, and photovoltaic materials.[3] Recent reports highlight the fact that variation of Stokes shift can be related to the strength of the ICT property and molecular geometry relaxation upon photoexcitation.[4] Several researchers have observed that compounds that exist in keto/enol tautomerisation display large Stokes shift and that these materials can be applied to various applications.[5]

2-Quinolinones, which are 2-pyridinone type molecular systems, have interesting structural and spectral properties due to their tendency to adopt tautomeric forms (keto and enol) that are nearly equal in energy.[6] Nishiwaki et al. have studied in detail the synthesis of quinolinone derivatives for biological applications,[7] and Natarajan et al. have synthesised several quinolinone-based metal complexes for anticancer activities.[8] However, some molecules with a keto/enol resonance unit suffer from poor solubility due to strong intermolecular H-bonding, which constrains their application in various fields.[9] Whereas introducing alkyl chains in the lactam units is an important approach to improving solubility,[10,9a,9b] introducing the substituents on the N- or O-atom of the quinolinone moiety will increase its solubility but may prevent the molecule from adopting its characteristic tautomer forms, which may influence the photophysical properties.

Despite intense research into the biological activities of quinolinone derivatives, to the best of our knowledge, no studies have focused on the quinolinone framework in

[a] School of Chemsitry, Bharathidasan University, Tiruchirappalli 620024, Tamilnadu, India
E-mail: rrengas@gmail.com
http://www.bdu.ac.in/schools/chemistry/chemistry/dr_r_renganathan.php

Supporting information for this article is available on the WWW under http://dx.doi.org/10.1002/ejoc.201301085.

donor–acceptor systems by precluding specific tautomer forms and analysing the effect on photophysical properties. In this context, we have chosen two types of quinolinone framework with three different acceptor groups. These two types of donor fragments are based on a common quinolinone moiety (Q) to which is attached a methyl (MQ) or a benzene moiety (BQ). Cyano acrylic acid (CA), nitrophenyl acetonitrile (NPAN), and Rhodanine acetic acid (RA) were introduced into the above quinolinone framework as acceptor moieties and the magnitude of acceptor parts in ICT properties were analysed. *N*- and *O*-alkylated quinolinone derivatives were synthesised to assess the impact of the tautomer on their optical properties. All the newly synthesised quinolinone compounds (Scheme 1) were characterised by ^{1}H NMR, ^{13}C NMR and mass analysis. Upon alkylation, striking differences were observed in the photophysical and Stokes shift properties of the derivatives. Furthermore, the electrochemical and thermal behaviour of the synthesised quinolinone compounds was analysed. Experimentally observed electronic properties of the quinolinone compounds were further examined by Density Functional Theory (DFT) and Time-Dependent DTF (TDDFT) calculations. The results gave deeper insights into factors affecting the structural and photophysical properties of quinolinone derivatives for both photovoltaic and biological applications.

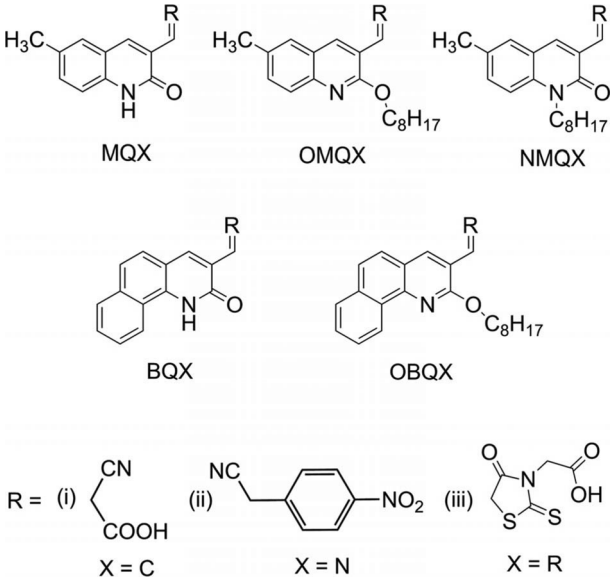

Scheme 1. Structures of unalkylated and *N*- and *O*-alkylated quinolinone compounds with various acceptor groups.

Results and Discussion

Synthesis and Characterisation of Quinolinone Compounds

The synthetic routes used for the preparation of unalkylated and *N*- and *O*-alkylated MQ and BQ compounds with various electron-withdrawing acceptor groups are depicted in Schemes 2 and 3. Aldehydes MQA and BQA were employed as common starting precursors for the synthesis of quinolinone-based donor acceptor compound. These starting materials were synthesised by following reported methods.[11,8b] The final compounds MQX and BQX (X = C, N, R) were conveniently prepared by the Knoevenagel condensation of MQA and BQA, respectively, by using the corresponding active methylene compounds as per literature procedures.[12] The characteristic –CH=C vinylic resonance band appeared around 8.4–9.3 ppm in the ^{1}H NMR spectra for all the compounds, which is consistent with previous reports.[12] The observed mass data further confirmed the identity of the final products.

The alkylation of BQA and MQA (Scheme 2), which was monitored by thin-layer chromatography (TLC), was carried out with 1-bromooctane in the presence of base (K_2CO_3) in *N*,*N*-dimethylformamide (DMF) and resulted in the formation of a mixture of NMQA, OMQA, and OBQA, respectively. TLC analysis of the reaction mixture obtained from alkylation of MQA revealed two spots [R_f (hexane/EtOAc, 1:0.1) = 0.6 (spot I), 0.2 (spot II)], whereas only one spot was detected for BQA [R_f (hexane/EtOAc, 1:0.1) = 0.76]. 2-Quinolinone type compounds are known

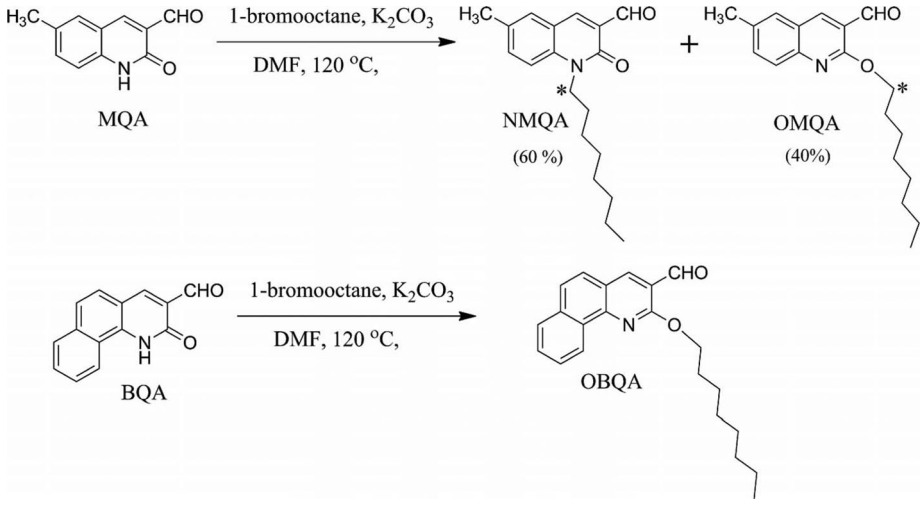

Scheme 2. Synthetic route used for the preparation of NMQA, OMQA, and OBQA.

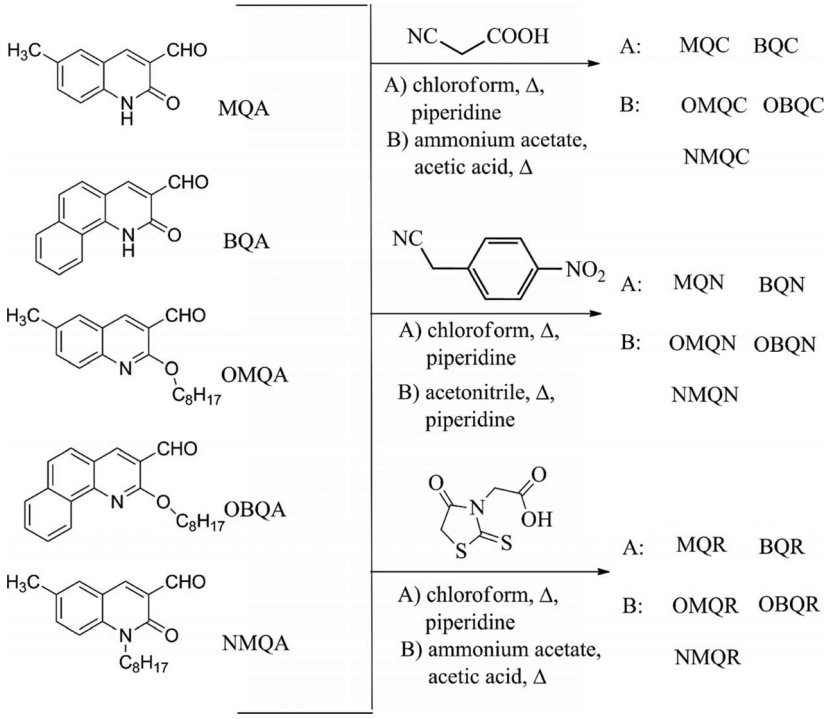

Scheme 3. Synthetic route used for the preparation of the 2-quinolinone derivatives with various electron-withdrawing groups.

to exist in equilibrium between keto and enol form, as shown in Scheme 4.[6] Hence, the alkylation of this type of compound involves an ambident anion that may result in mixtures of *N*- and *O*-alkylated products.[13] Based on this, the formation of two spots in the alkylation of MQA may correspond to the formation of both *N*- and *O*-alkylated products, whereas either the *N*- or *O*-alkylated isomer was formed in the alkylation of BQA. ^{1}H NMR spectroscopic analysis of the compounds forming spots I and II from the alkylation reaction of MQA (see the Supporting Information, SI2 and SI4, respectively) reveal only slight variations, which made identification of the corresponding product difficult. However, the ^{13}C NMR spectra of the compounds making up spots I and II (see the Supporting Information, SI5) were significantly different, with a major difference being observed in the region 40–70 ppm. Spot I material gave rise to a signal at ca. 66 ppm, whereas this was absent in the spectrum obtained from spot II, with the latter having a signal at ca. 42 ppm. When comparing the *N*- and *O*-alkylated MQ quinolinone compound (see the Supporting Information, SI5), the alkyl carbon (marked with an asterisk) attached to the oxygen atom should appear more downfield than when attached to a nitrogen atom, the electronegativity of which is less than oxygen. Hence, the material generating a ^{13}C NMR signal at ca. 66 ppm should correspond to the *O*-alkylated product. Accordingly, spot II was assigned as the *N*-alkylated product. The product obtained in the alkylation of BQA also possesses a signal at ca. 66 ppm and was accordingly assigned as *O*-alkylated BQA. Recently, Torhan et al. reported the relationship between the ratio of *N*- and *O*-alkylation products and the nature of substituents in 2-pyridone type compounds.[13m] MQ and BQ series differed in the methyl and benzene substituent in the common quinolinone moiety and this substituent effect is one of the reasons for the formation of preferred *N*-/*O*-alkylated products.

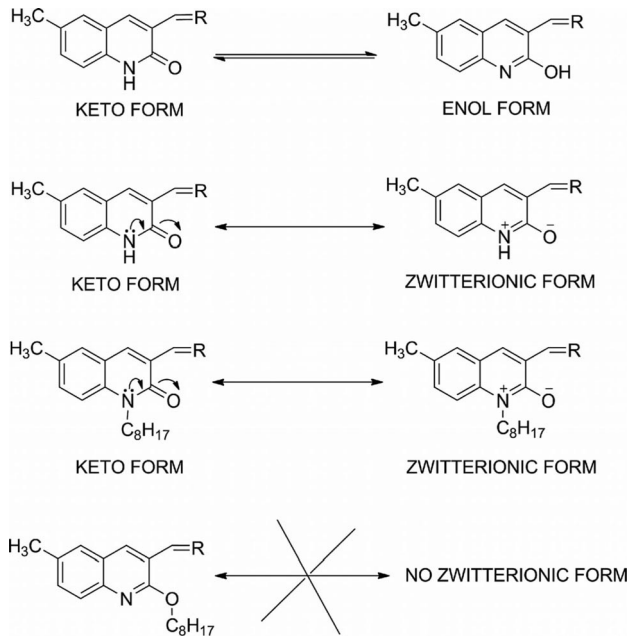

Scheme 4. Possible equilibrium and resonance forms of unalkylated and N/*O*-alkylated quinolinone compounds. "R" represents the various acceptor groups.

The assignment of spot I as the *O*-alkylated compounds by using NMR techniques was confirmed by single-crystal XRD structure analysis of OBQA.[14] A needle-like crystal

was obtained from alkylated BQA in dichloromethane/methanol solvent. The single-crystal X-ray structure of this compound (Figure 1, A; for details of crystal data see the Supporting Information, SI20) revealed that OBQA crystallized in a triclinic crystal system in the P-1 space group. Due to the presence of alkyl chains, the possibility of π-π stacking in the benzene-fused quinolinone is prevented, which is clearly observed from the crystal packing (Figure 1, B). The obtained alkylated aldehydes were subjected to Knoevenagel condensation to give the final products (OMQX, NMQX, OBQX, X = C, N, R). All the alkylated products were characterised by ^{1}H NMR, ^{13}C NMR and mass analysis.

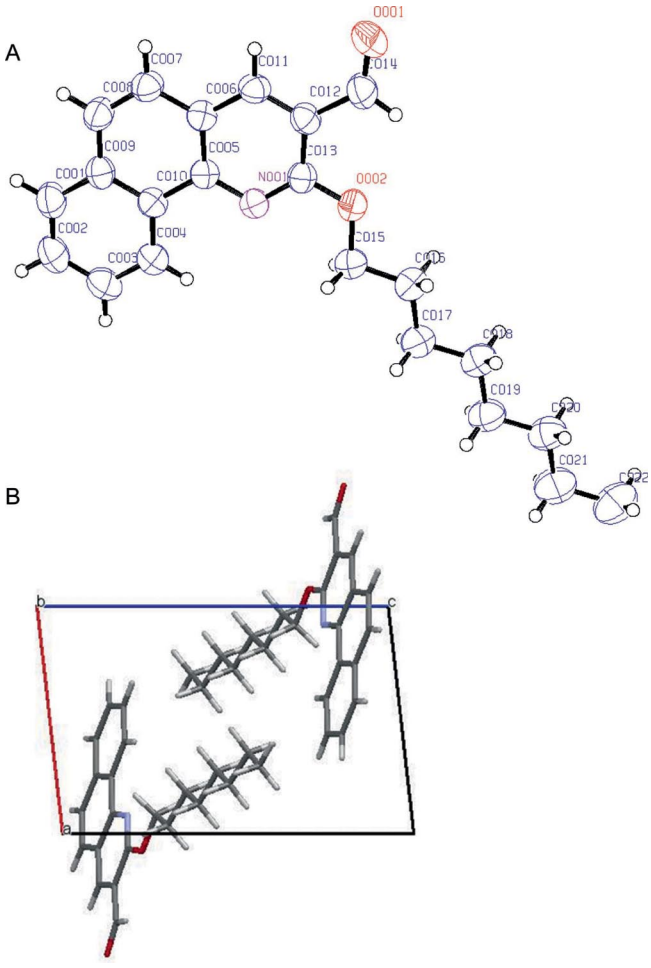

Figure 1. (A) Single-crystal X-ray structure of OBQA. (B) Crystal packing view of OBQA along the *b*-axis.

Electronic Properties

The absorption spectra in tetrahydrofuran (THF) of MQ and BQ derivatives substituted with various electron-withdrawing groups are presented in Figure 2, and the relevant data are summarised in Table 1. Compared with methyl- (MQ) and benzene- (BQ) substituted quinolinone derivatives, the absorption of BQ derivatives appeared in the higher wavelength region due to the presence of the extra conjugation system in the benzene ring. All the compounds exhibit a high-energy absorption band around 300–400 nm, which arises due to π→π* transitions[15] and a second band in the visible region (400–500 nm). Fine tuning of the absorption characteristics of these compounds was observed by introducing different acceptor groups. The visible absorption of MQC and MQN appears at 417 and 418 nm, respectively, whereas the absorption of MQR falls at 434 nm. Although, the conjugated system was larger in MQN, MQC has a similar absorption region. This implies that during the photoexcitation, the electron density around the quinolinone moiety shifts towards the electron-withdrawing (EW) cyano group in MQC. MQR shows a further bathochromic shift, reflecting the strong electron-withdrawing capability of the rhodanine group. As a result, the localisation of π→π* transition over the acceptor group (charge-transfer transition) was enhanced by introducing the electron-withdrawing groups. Hence, the band that appears in the visible region is due to charge-transfer transitions, as observed in earlier reports.[16] Thus, the band around 300–400 nm stems from π→π* transition localising on the quinolinone segment, whereas the visible band originates from π→π* transition extended over the acceptor segment.[17] Furthermore, the absence of a band in the visible region for the absorption of MQA (strong acceptor group is absent) supports the origin of charge-transfer transitions being due to the presence of an acceptor group. In the case of BQ derivatives, the BQR absorption appears at 473 nm, whereas those of BQC and BQN have maximum

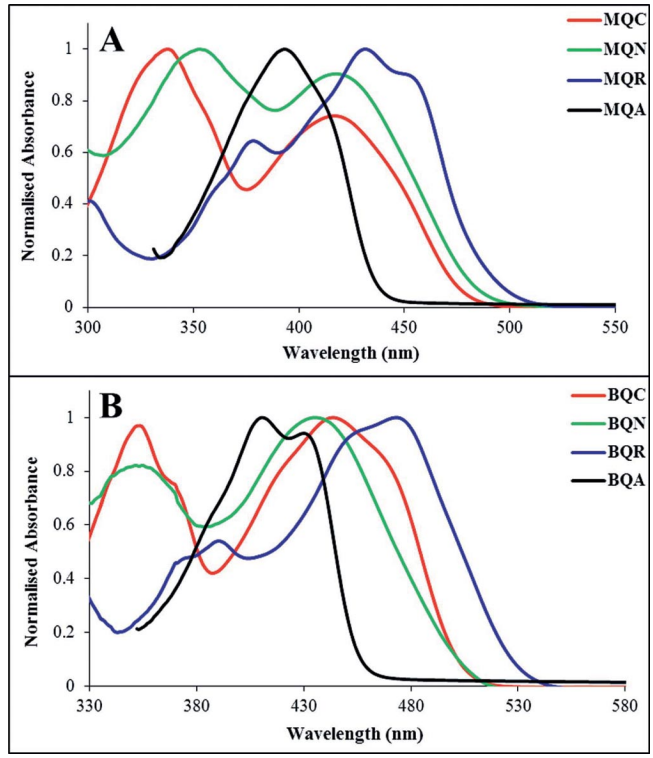

Figure 2. Absorption spectra of unalkylated (A) MQX, and (B) BQX compounds recorded in THF solvent [X = C, N, R (1×10^{-4} M)].

Table 1. Photophysical data of unalkylated and *N*- and *O*-alkylated quinolinone compounds substituted with various acceptor groups (THF solvent).

	MQC	MQN	MQR	BQC	BQN	BQR	OMQC	OMQN	OMQR	OBQC	OBQN	OBQR	NMQC	NMQN	NMQR
λ_{abs} [nm]	417	418	431	444	435	473	332	358	397	336	346	419	402	416	430
Absorption coefficient[a]	3.22	1.64	3.56	0.17	1.67	2.32	0.81	1.68	2.79	0.61	0.68	1.74	0.64	1.2	2.8
λ_{emi} [nm]	524	538	521	522	536	529	463	493	491	490	517	499	510	535	520
Stokes shift[b]	4896	5336	4007	3365	4331	2238	8522	7648	4822	4908	9559	3826	5267	5346	4025
Quantum yield (ϕ_f)	0.61	0.51	0.35	0.69	0.67	0.51	0.51	0.32	0.14	0.68	0.66	0.15	0.57	0.55	0.19

[a] ε [10^4 M^{-1} cm^{-1}]. [b] $\Delta\nu$ [cm^{-1}].

absorptions at 444 and 435 nm, respectively. These different acceptor groups have similar effects on the absorption trend for MQ and BQ derivatives. Comparatively, the RA moiety possesses greater electron-withdrawing capability than the other acceptor groups, whereas the CA moiety has comparable electron-withdrawing character to that of the NPAN acceptor. The observed absorption behaviour illustrates the importance of incorporating acceptor groups in the quinolinone core structure to tune their optical properties.

The absorption behaviour of *O*-alkylated BQ derivatives in comparison to their unalkylated BQ derivatives is displayed in Figure 3 and the data is summarised in Table 1. Comparing the absorption characteristics of BQC and OBQC, the CT band around 444 nm for the former was completely absent and the peak corresponding to $\pi \rightarrow \pi^*$ transition localised on the quinolinone segment was more prominent. A similar disappearance of a CT band was observed for OBQN. For RA substituted compounds the band was shifted to a lower wavelength region. Similar behaviour was observed for all OMQ compounds. The observed optical properties of the *O*-alkylated MQX and BQX (X = C, N, R) compounds reveal that alkylation at the O-position prevents charge-transfer transition behaviour of the quinolinone derivatives. This assumption was further supported by analysing the absorption behaviour of *N*-alkylated MQ compounds. The absorption spectra of the NMQ series in THF solvent (Figure 3, Table 1) clearly show that the absorption behaviour of *N*-alkylated compounds retains the

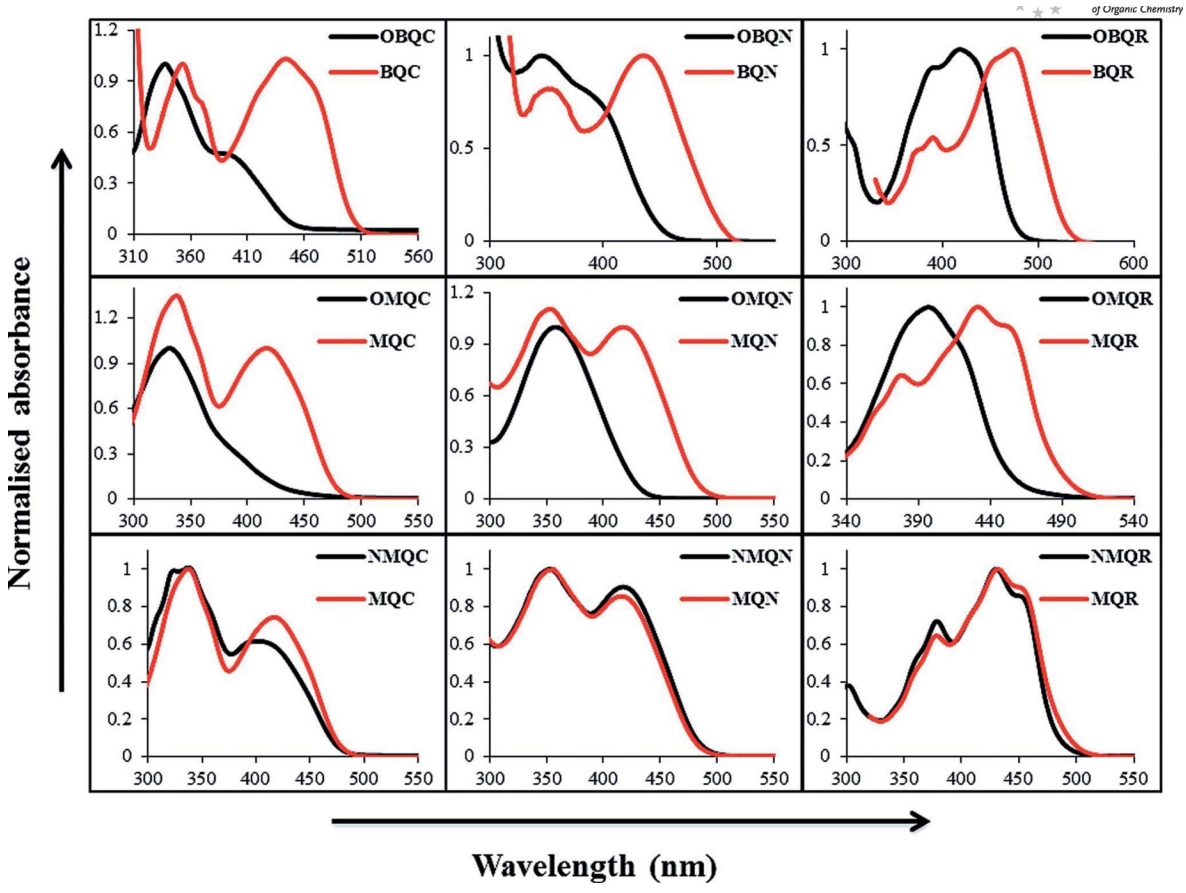

Figure 3. Absorption spectra of alkylated OBQX, OMQX and NMQX (X = C, N, R) along with the absorption spectra of their respective unalkylated compounds recorded in THF.

CT transitions, as observed in unalkylated MQ compounds. This observation suggests that alkylation on the nitrogen atom does not lead to any significant change in the CT absorption behaviour of the quinolinone compounds. These trends signify that the optical properties of 2-quinolinone type derivatives can be easily tuned by varying the alkylation at the N- or O-position.

The possible tautomer structures of unalkylated, *N*-alkylated, and *O*-alkylated quinolinones are shown in Scheme 4. Nimlos et al. calculated the C–N bond length of the lactam tautomer of 2-hydroxy quinoline by using semiempirical methods and obtained a value (1.39 Å) that lies between those of the neutral and zwitterionic form, indicating significant contributions from both tautomer structures.[6a] To unravel the structural properties of these molecules, DFT calculations were carried out at the B3LYP/6-31g(d) level. All these molecules have a rigid quinolinone unit and the acceptor and alkyl groups are slightly twisted out of the quinolinone plane. The important bond lengths, listed in Table 2, show that the C–N bond lengths of unalkylated and *N*-alkylated quinolinones fall between those of C–N single (1.47 Å) and double (1.29 Å) bonds. This implies that these structures have excellent delocalisation and that the unalkylated and *N*-alkylated quinolinones favour zwitterionic forms, as previously reported.[6a] However, the C–N bond lengths of *O*-alkylated quinolinone compounds were found to be closer to those of a double bond, thus favouring the neutral structure over the zwitterionic form. Based on this observation, unalkylated quinolinone apparently exists in equilibrium between the keto (lactam) and enol (lactim) form. Furthermore, the lactam form can also exist in a zwitterionic resonance structure.[6] *N*-Alkylated quinolinones also have the possibility of existing in zwitterionic forms.[18] However, *O*-alkylated quinolinones can be represented in one form and there is no available zwitterionic resonance structure. These different forms reveal that the common possible structure among the unsubstituted and *N*-alkylated quinolinones is the zwitterionic form. The aromatic π density is delocalised over the oxygen atom in the resonance zwitterionic form, which increases the extent of the π-system and creates a higher electron density around the pyridinone moiety.[6] During photoexcitation, this higher electron density is attracted by the electron-withdrawing groups, and the localisation of the $\pi \rightarrow \pi^*$ transition extends over the acceptor groups, resulting in prominent CT bands in the visible region, similar to previous reports.[6a] As a result of the absence of a resonance zwitterionic form in *O*-alkylated quinolinone compounds, no such extra electron density around the oxygen atom exists, leading to the absence of a prominent CT transition. The molar extinction coefficient (ε [$M^{-1}\,cm^{-1}$]) of these quinolinone compounds usually provides information on their light-harvesting efficiency and their suitability for further application in photovoltaic applications.[2q,2r] The ε values of all the compounds under investigation were calculated at their absorption maxima (in THF) and are listed in Table 1 (see the Supporting Information, SI25 for ε values in other solvents). The observed ε values of all the compounds were found to be sufficient for their use in photovoltaic applications. Among the various acceptor groups, RA-substituted quinolinone had the highest ε, with the lowest ε values being found for CA substituted compounds.

Table 2. B3LYP/6-31g(d) optimised C–N and C–O bond lengths [Å].

Compound	C–N	C–O	Compound	C–N	C–O
BQC	1.39849	1.22622	O-MQC	1.30719	1.34754
BQN	1.39575	1.22782	O-MQN	1.30654	1.34994
BQR	1.39615	1.22769	O-MQR	1.30610	1.35000
MQC	1.39256	1.22612	N-MQC	1.40659	1.22899
MQN	1.39012	1.22772	N-MQN	1.40265	1.23169
MQR	1.39073	1.22758	N-MQR	1.40326	1.23148
O-BQC	1.31232	1.34627			
O-BQN	1.31149	1.34890			
O-BQR	1.31109	1.34892			

Excited State Properties

The emission spectra of all the quinolinone derivatives in THF are shown in Figure 4 and the related data are gathered in Table 1. Based on the ground-state optical properties, it is more pertinent to analyse the excited properties in two different ways, such as influence of acceptor groups and effect of alkylation. By varying the acceptor groups, a difference in the excited behaviour of the quinolinone compounds was observed. The BQ series containing different acceptor groups showed emission trends as follows: BQN > BQR > BQC. In contrast in the observed absorption trend, BQR shows more blueshifted emission behaviour than BQN. Similarly, MQN shows lower energy emission behaviour than MQR and MQC. In the alkylated quinolinone series, compounds having a NPAN segment have redshifted emission behaviour. The observations from the excited state behaviour points to the fact that the NPAN acceptor segment has more extensive conjugation than other EW groups, which is reflected in the emission properties of these quinolinone compounds, as discussed in previous reports.[19] Comparing the unalkylated and *N*-alkylated MQ compounds, similar emission behaviour is observed that is analogous to their ground state properties. As predicted from the absorption behaviour, the emission maxima of the *O*-alkylated quinolinone compounds appear at lower wavelength regions compared with those of the *N*-alkylated and unalkylated derivatives. The excitation spectrum of these compounds was measured to gain further information on the nature of the emission behaviour and the spectra are displayed in the Supporting Information (SI26). Unalkylated and alkylated compounds have both $\pi \rightarrow \pi^*$ conjugation and charger transfer bands in their excitation spectra, whereas only $\pi \rightarrow \pi^*$ conjugation bands are observed for the *O*-alkylated series. The excitation spectra of all the compounds reflect their absorption behaviour. This implies that the emission is not purely a result of charge transfer characteristics and supports the contribution of "π" conjugation in the excited state, as stated for NPAN acceptor com-

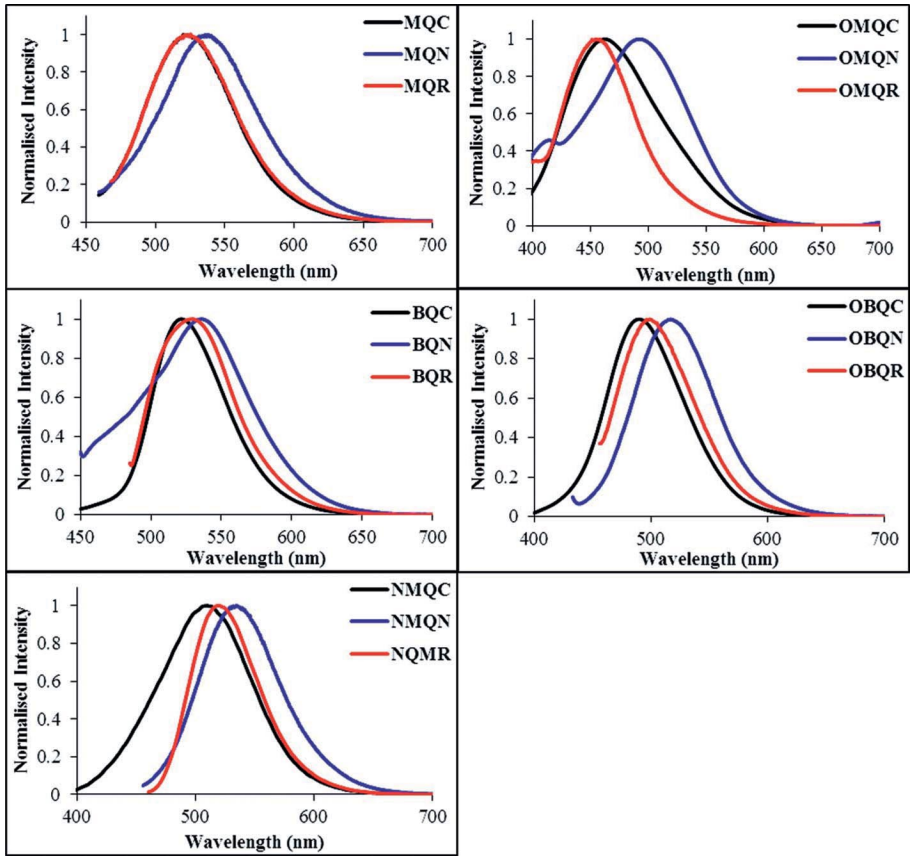

Figure 4. Emission spectra of unalkylated and *N*- and *O*-alkylated MQX and BQX compounds recorded in THF (X = C, N, R).

pounds. The fluorescence quantum yields of the quinolinone compounds were measured in THF solvent and the values are given in Table 1. These observed values reveal that the quantum yield of these quinolinone compounds depend on the EW acceptor part. For example, the quantum yield of MQC is 0.61 but it is reduced to 0.35 for MQR. Similarly, the quantum yield of OBQC and OBQR are 0.68 and 0.15, respectively. In general, the CA acceptor substituted quinolinone compounds show higher quantum yield (ϕ = 0.69) whereas the quantum yield is very low with RA acceptor compounds. Compounds with the NPAN acceptor have comparable quantum yields to those with the CA acceptor. The observed difference in the quantum yield depending on the acceptor part is similar to those noted in our recent report.[2s] There was no significant difference in the quantum yield among alkylated and unalkylated quinolinone compounds.

The Stokes shift of these compounds in THF are summarised in Table 1 and those of all compounds in various solvents are given in the Supporting Information (SI25). Among the different acceptor groups, NPAN substituted compounds have relatively large Stokes shift in various solvents. The Stokes shifts of all compounds in THF solvent followed the order: MQN > MQC > MQR, BQN > BQC > BQR, OMQN > OMQC > OMQR, NMQN > NMQC > NMQR, OBQN > OBQC > OBQR, which highlights the small Stokes shift observed for RA substituted compounds. Interestingly, the Stokes shifts for the *O*-alkylated series is larger than for other compounds. For example, the Stokes shift of BQN in DMF solvent is 2206 cm^{-1}, whereas upon *O*-alkylation (OBQN), the Stokes shift increased dramatically to 9684 cm^{-1}. Similarly, a 4331 cm^{-1} Stokes shift of BQN in THF solvent is increased to 9559 cm^{-1} for OBQN. DFT studies reveal that the excited state of *O*-alkylated structures is perturbed more than the corresponding *N*-alkylated and unalkylated compounds. This leads to the existence of nonradiative relaxation pathways such as structural reorganisation in the excited state and results in a large Stokes shift.[3,17] The obtained large Stokes shift values are analogous with the recently reported molecules,[3b,3d,3e] and such compounds can diminish the inner filter effect, which suggests the possible application of these compounds as biological fluorescent probes.[3d,3e,3g]

Solvatochromism

The absorption and emission spectra in various solvents were measured to gain more information regarding the solvent effect on the photophysical properties of the quinolinone compounds. The representative figures are shown in the Supporting Information (SI21–SI24) together with a summary of the relevant data (SI 25). A comparison of the absorption and emission behaviour of all quinolinone com-

pounds in various solvents (see the Supporting Information, SI27) clearly reveals that the absorption of the RA acceptor group substituted quinolinone compounds has more redshifted absorption than other acceptor groups in various solvents. Unalkylated and *N*-alkylated compounds have more extensive changes in absorption characteristics in various solvents than *O*-alkylated compounds. As discussed above, NPAN acceptor group substituted compounds shows redshifted emission behaviour compared with other acceptor groups. Compared to their ground state, the excited state of these compounds is more sensitive to changes in solvent. A positive solvatochromism is expected if the emission behaviour is related to ICT,[20] however, the fact that there is no clear trend observed on increasing the solvent polarity points to the involvement of other factors. A better description of the solvent effect in both the ground and electronic excited states of the compounds was attempted by using the Lippert–Mataga equation.[21] The Lippert–Mataga plot of Stokes shift and orientation polarisability of solvents for all the quinolinone derivatives (see the Supporting Information, SI28) reveals a nonlinearity of the Lippert–Mataga correlation, which shows the existence of specific solvent effects.[22] Factors such as hydrogen-bonding and polarisability are potential causes of the observed solvent effect, as discussed in the literature.[23] The use of the Reichardt–Dimroth polarity parameter $E_T(30)$ is another important method with which to gain a better understanding on the solvatochromic behaviour of the quinolinone compounds.[24] The correlation of Stokes shift with the $E_T(30)$ parameter for all the quinolinone compounds (see the Supporting Information, SI29) reveals a deviation from linearity, indicating the involvement of solute–solvent interactions other than dipole–dipole (charge transfer) interactions in the excited state of the compounds.

Electrochemical Properties

The electrochemical behaviour of the quinolinone compounds was scrutinised by using cyclic voltammetry and differential pulse voltammetry measurements; the voltammograms of the quinolinone compounds are displayed in Figure 5 for the MQ series (see the Supporting Information, SI30 for other compounds) and the data are listed in Table 3. The unalkylated quinolinone compounds exhibit quasireversible oxidation processes, whereas irreversible oxidation is observed for the alkylated compounds. Among the various acceptor groups, the oxidation of the unsubstituted quinolinone with the RA acceptor group occurs at higher potential, which signifies the strongest accepting behaviour by the rhodanine moiety. An anodic shift in the oxidation of alkylated compounds was observed relative to unalkylated compounds. The oxidation of *N*-alkylated compounds was cathodically shifted compared with *O*-alkylated derivatives. The introduction of alkyl chains onto the quinolinone compounds results in tuning the HOMO energy level by 300 mV, as can be predicted from the potentials of all the compounds. This difference in the oxidation of the alkylated and unalkylated compounds suggests that the oxidation process is mainly centred on the pyridinone moiety. The reduction behaviour of these compounds (Table 3 and the Supporting Information, SI30) show that among the different acceptor groups, the reduction potential of RA acceptor substituted unalkylated and *N*-alkylated compounds shifts towards more positive values, whereas the *O*-alkylated compounds with a CA acceptor part have more positive reduction behaviour. The reduction potential for MQC (–0.95 V) remains almost the same as for its *N*-alkylated counterpart (NMQC, –0.92 V), whereas it was altered for OMQC (–0.85 V). Overall, the reduction behaviour of alkylated and *N*-alkylated series behave in a similar manner. These observations further suggest that the incorporation of acceptor groups and alkylation in the pyridinone moiety plays an important role in tuning the energy levels of the quinolinone-based compounds.

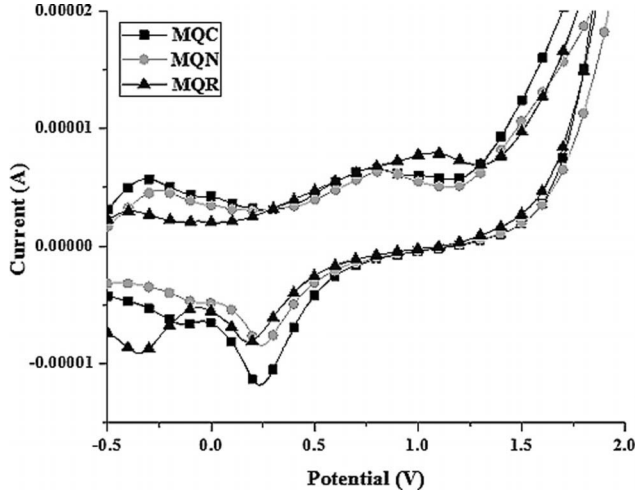

Figure 5. Cyclic voltammograms of MQX (X = C, N, R) recorded in THF (vs. AgCl/Ag electrode).

Table 3. Electro-optical data of the quinolinone compounds.

	E_{ox} [V][a]	E_s [eV][b]	E_{ox*} [eV][c]	E_{red} [V][a]
MQC	0.78	2.97	–2.19	0.95
MQN	0.84	2.64	–1.8	0.87
MQR	1.08	2.59	–1.51	0.85
BQC	0.84	2.71	–1.87	0.87
BQN	0.83	2.64	–1.81	0.80
BQR	1.05	2.50	–1.45	0.85
OMQC	1.19	3.08	–1.89	0.85
OMQN	1.24	3.05	–1.81	0.86
OMQR	1.21	2.90	–1.69	0.99
OBQC	1.34	3.02	–1.68	0.78
OBQN	1.33	2.85	–1.52	0.93
OBQR	1.23	2.74	–1.51	0.97
NMQC	1.1	2.92	–1.82	0.92
NMQN	1.2	2.61	–1.41	0.85
NMQR	1.25	2.62	–1.36	0.83

[a] Oxidation potential (E_{ox}) and reduction potential (E_{red}) of the quinolinone compounds (10^{-3} M) in DMF containing 0.1 M tetrabutylammonium hexafluorophosphate (vs. AgCl/Ag electrode). [b] E_s was calculated from the intersection of absorption and emission in DMF. [c] $E_{ox*} = E_{ox} - E_s$.

EurJOC European Journal of Organic Chemistry

Thermal Properties

Thermogravimetric analysis (TGA) was performed to investigate the thermal stability of the quinolinone compounds (see the Supporting Information, SI31). All the compounds exhibit good thermal stability and temperatures corresponding to 5% weight loss (T_d) for the MQ and BQ compounds with various acceptor groups were 250 (MQC), 320 (MQN), 290 (MQR), 233 (BQC), 310 (BQN), and 298 °C (BQR). Among the different acceptor groups, CA exhibited lower T_d, whereas quinolinones with the NPAN group showed higher thermal stability relative to RA. This is due to the presence of a –COOH group in CA and RA, which leads to a decarboxylation process as reported previously[25] and lowers its T_d compared with NPAN derivatives. To examine the alkylation effect, the TGA of OMQR, NMQR and OBQR was analysed and their T_d values were found to be 327, 324 and 322 °C, respectively, which were higher than their parent unalkylated compounds. The stability of the alkylated compounds was comparable to quinolinone compounds with the NPAN group. The observed thermal stability data suggests these quinolinone compounds are suitable for use in various photovoltaic applications.

Theoretical Insights into the Optical and Electrochemical Properties

Frontier molecular orbitals are often used to obtain qualitative information about the optical and electrochemical properties of molecules. To understand the reactivity, the frontier molecular orbitals and their corresponding energy levels have been examined (see the Supporting Information, SI32–SI34). The frontier molecular orbital (HOMO and LUMO) pictures of MQ derivatives are depicted in Figure 6 (see also the Supporting Information, SI32 and SI33). From these calculations it is clear that the HOMO is delocalised over the entire quinolinone unit and is extended slightly into the acceptor part. The LUMO is evenly delocalized on the acceptor group, and part of quinolinone unit is also involved. The alkyl group takes part in neither HOMO nor LUMO orbitals. Furthermore, the frontier molecular orbitals show that both the HOMO and LUMO levels of all these molecules have π character and are stabilized by the acceptor groups. Hence, the electronic transitions of these molecules arise from both intramolecular charge-transfer (CT) and $\pi \rightarrow \pi^*$ transitions.

To gain further insights from these frontier molecular orbitals, energetics of the HOMOs and LUMOs and their corresponding compositions were computed by using the QMForge program.[26] The compositions of the HOMO and LUMO orbitals were partitioned according to the contribution from the quinolinone unit, the acceptor unit and the alkyl group, and the results are presented in Figure 7 (see also the Supporting Information, SI34). It is clear from these calculations that the contribution of the quinolinone unit to the HOMO gradually decreased from 86 to 45% upon moving from MQC to MQR. At the same time, in

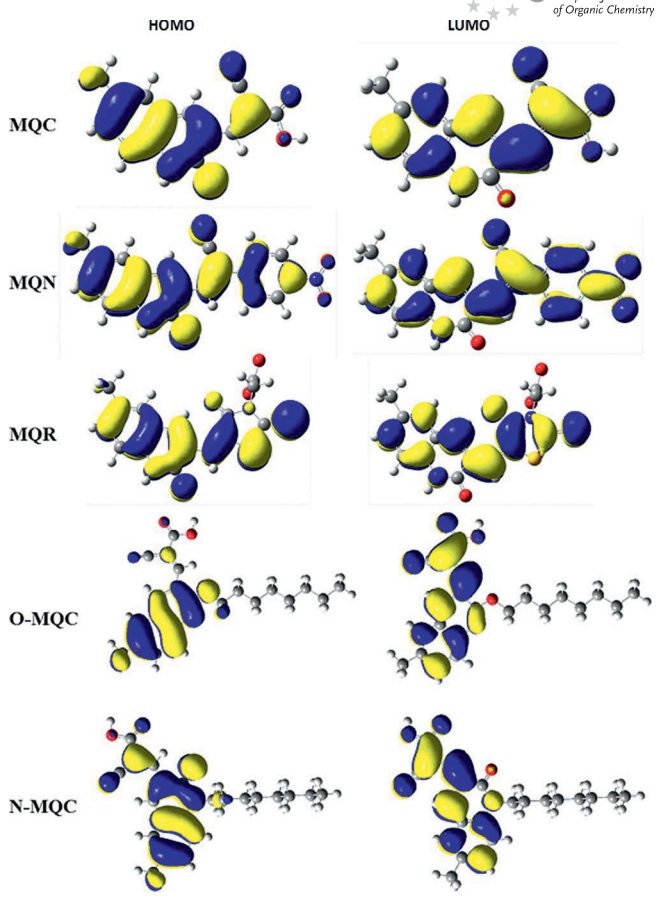

Figure 6. Frontier molecular orbitals (HOMO and LUMO) of MQC, MQN, MQR, NMQC and OMQC.

MQC, a 14% contribution of the acceptor towards the HOMO is significantly increased to 46%. Furthermore, the quinolinone unit contributes 94 and 85% to HOMO in OMQC and NMQC, whereas it reduced to 44 and 53%, respectively, towards the LUMO. As evident from the molecular orbital diagrams of the BQ derivative, the contribution of the quinolinone unit predominates (60–90%) in the HOMO, whereas the contribution of the acceptor groups improved 30–40%. It is important to note that quinolinone derivatives with a CA acceptor group have ca. 90% HOMO contribution from the quinolinone unit, whereas the acceptor group contributes very little (< 12%); for the LUMO, the contribution of the acceptor group increases to 55%. The HOMO of RA substituted quinolinone gets greater contributions from both the quinolinone unit as well as the acceptor group. However, contributions from the alkyl group in *N*- and *O*-alkylated compounds towards HOMO and LUMO is up to 3 and 1%, respectively. This analysis provides further useful clues for the design of such molecules with various acceptor groups for use as improved candidates for optoelectronic applications.

Time-dependent DFT (TDDFT) calculations have been carried out on the ground state geometries to understand and explain the nature of transitions for the observed absorption spectra of these molecules. The details of the excitation energies, oscillator strength (*f*), and contributing con-

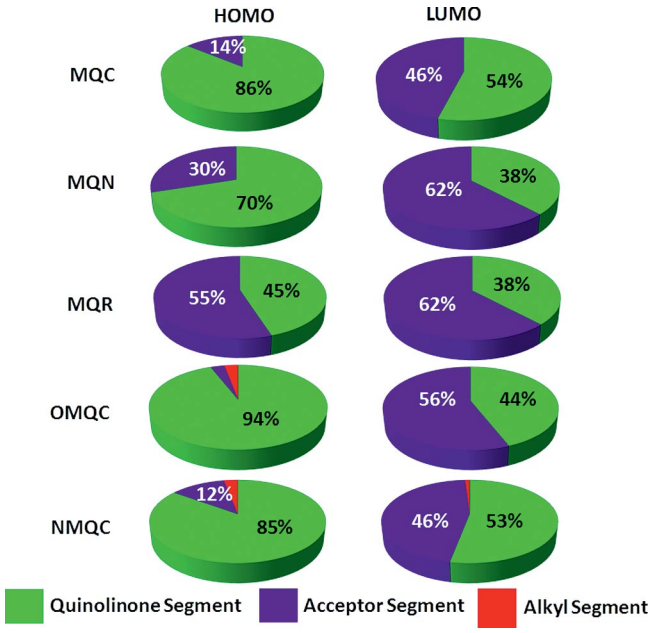

Figure 7. Percentage contribution from different segments towards the HOMO and LUMO.

figurations for the most probable electronic transition of all the molecules in THF are summarised in the Supporting Information (SI35). In line with the experiments, two absorption bands were predicted in the range of 300–400 and 400–500 nm. The strongest absorption was observed at 372 and 482 nm for BQC, which arise from HOMO–1 → LUMO (85%) and HOMO → LUMO (85%), respectively. RA substituted quinolinone compounds were found to display redshifted absorption compared with other acceptor groups, as expected from experimental observations. As seen from the frontier molecular orbital diagrams, the distribution of HOMO and LUMO in these molecules has a significant overlap, which implies that the transitions are from both the charge transfer as well as π-π* transitions.[17b] MQN displays an intense absorption peak at 472 nm with an excitation energy of 2.63 eV. This peak was mainly due to HOMO → LUMO (85%) transition with oscillator strength of 0.5652. Another interesting fact is that the HOMO–1 → LUMO transitions are responsible for the peak around 300–400 nm, whereas the peak obtained between 400–500 nm originates from HOMO → LUMO transitions. In line with experiments, O-MQC possesses the lowest absorption (362 nm) among all, and was assigned to the HOMO → LUMO (98%) transition with an oscillator strength of 0.6739. The absorption wavelength of the quinolinone compounds increases upon moving from CA, NPAN to RA acceptor group, respectively, which is in good agreement with experimentally observed absorption properties.

Conclusions

A series of quinolinone core structures with different acceptor and alkylated groups were synthesised and characterised by ^{1}H NMR, ^{13}C NMR and mass analysis. The significance of these modifications on the photophysical properties of the quinolinone moiety was investigated by using a range of experimental and theoretical techniques. Charge-transfer transitions in the visible region were observed by introducing electron-withdrawing acceptor groups to the quinolinone framework. Among the different acceptor groups, rhodanine acetic acid substituted quinolinone showed better electron-withdrawing property as indicated by the more redshifted absorption. A significant change in the quinolinone photophysical properties was observed between *N*- and *O*-alkylated compounds. The observed photophysical properties among different compounds reveal that the presence of zwitterionic resonance structures play a crucial role in the charge-transfer behaviour. TDDFT studies clearly predict the absorption trend and accounts for the nature of the transitions. The Stokes shift of the *O*-alkylated quinolinone was found to be larger among unalkylated and *N*-alkylated quinolinone compounds. The higher quantum yield of these quinolinone-type compounds facilitates their use in biological applications. The combination of acceptor groups and alkylation on the pyridinone moiety plays an important role in tuning the energy levels of the quinolinone-based compounds. Theoretical studies suggest that the contribution of the quinolinone unit predominates in the HOMO, whereas the LUMO is delocalised onto the acceptor fragments. The observed good thermal stability for all the compounds makes them suitable candidates for use in photovoltaic applications. Considering the above results, such as altered photophysical properties by a simple change in alkylation position, large Stokes shift, tunable electrochemical behaviour, and good thermal behaviour, signifies that quinolinone-based compounds should emerge as potential candidates for photovoltaic and biological applications. Furthermore, the observed results delineate the factors that determine the photophysical properties of quinolinone derivatives and should allow better molecular engineering to tune the structural and photophysical properties of such compounds towards various applications. Synthesis of a range of quinolinone-based donor and acceptor systems with potential use in photovoltaic and biological applications are in progress in our laboratory.

Experimental Section

Chemicals and Instrumentation: Phosphorous oxychloride, dimethyl formamide, octyl bromide, rhodanine acetic acid, 4-nitrophenylacetonitrile, and piperidine were purchased from Sigma–Aldrich. 4-Bromo aniline, acetyl chloride, cyanoacetic acid, ammonium acetate, and acetic acid were purchased from LOBA chemicals. All solvents were of Analar reagent grade and used as received. ^{1}H and ^{13}C NMR spectra were obtained with a Bruker spectrometer operating at 400 MHz and 100 MHz, respectively. Mass spectra were obtained with a Bruker Daltonics, FT-ICR/APEX II, operating in ESI mode. Absorption spectral measurements were recorded with a JASCO V630 UV/Visible spectrophotometer. Fluorescence and excitation measurements were carried out with a JASCO FP-6500 spectrofluorimeter. Fluorescence quantum yield was calculated by using the equation: $\Phi_s = \Phi_r [(I_s/A_s)/(I_r/A_r)]$

$(\eta_s/\eta_r)^2$, where Φ_r and Φ_s are the quantum yield of the reference and sample. Perylene (Φ = 0.94) and diphenyl anthracene (Φ = 0.93) in cyclohexane was used as reference. I_r and I_s are the integrated photoluminescence area for the reference and sample, respectively. A_r and A_s are the absorbance of the reference and sample at the excitation wavelengths, and η_r and η_s are the refractive indexes of the solvents used for reference and sample, respectively. Cyclic voltammetry and differential pulse voltammetry (DPV) measurements were carried out with Princeton Applied Research, Versastat II instruments in dimethyl formamide medium. Tetrabutylammonium hexafluorophosphate (0.1 M) was used as supporting electrolyte. The experimental setup consisted of a platinum working electrode, platinum wire counter electrode and a silver/silver chloride reference electrode. All samples were deaerated by bubbling with pure nitrogen gas for ca. 5 min at room temperature. Thermogravimetric analyses (TGA) were performed at a heating rate of 10 °C/min. Thin-layer chromatography (TLC) was carried out on aluminium sheets pre-coated with silica gel 60F254 (E. Merck). Crystallographic data collection was performed with a Bruker kappa Apex II CCD detector system and single-crystal X-ray diffractometer equipped with a fine-focus sealed X-ray tube using graphite-monochromated Mo-K_α radiation (λ = 0.71073 Å). Structure solution and refinement were carried out by using the SHELXL-97 software package. All calculations were performed by using the WINGX software package and SHELX programme.

General Procedure for the Preparation of MQX and BQX (X = C, N, R) Compounds: To a mixture of quinolinone aldehyde (MQA or BQA) (1 equiv.) and the corresponding active methylene compound (1 equiv.) in chloroform, piperidine (0.01 equiv.) was added and the mixture was heated to reflux until TLC analysis showed the disappearance of the aldehyde spot. After the completion of the reaction, the precipitated solid was filtered and dried in vacuo to yield the desired product.

2-Cyano-3-(6-methyl-2-oxo-1,2-dihydroquinolin-3-yl)acrylic Acid (MQC): Yield 76%. ^{1}H NMR (400 MHz, [D$_6$]DMSO): δ = 12.24 (s, 1 H), 8.77 (s, 1 H), 8.46 (d, J = 5.6 Hz, 1 H), 7.59 (s, 1 H), 7.49 (d, J = 6.8 Hz, 1 H), 7.27 (d, J = 8.4 Hz, 1 H), 2.36 (s, 3 H) ppm. ^{13}C NMR (100 MHz, [D$_6$]DMSO): δ = 162.9, 160.0, 147.7, 140.9, 138.1, 134.7, 131.9, 128.8, 123.4, 118.1, 115.7, 115.3, 104.7, 20.1 ppm. HRMS (ESI): calcd. for [M + H]$^+$ 255.0769; found 255.0765.

3-(6-Methyl-2-oxo-1,2-dihydroquinolin-3-yl)-2-(4-nitrophenyl)-acrylonitrile (MQN): Yield 90%. ^{1}H NMR (400 MHz, [D$_6$]-DMSO): δ = 12.22 (s, 1 H), 8.68 (s, 1 H), 8.35 (d, J = 8.8 Hz, 2 H), 8.22 (s, 1 H), 8.02 (d, J = 8.8 Hz, 2 H), 7.59 (s, 1 H), 7.46 (d, J = 8.0 Hz, 1 H), 7.27 (d, J = 8.4 Hz, 1 H), 2.37 (s, 3 H) ppm. ^{13}C NMR (100 MHz, [D$_6$]DMSO): δ = 160.4, 140.5, 139.3, 137.4, 133.8, 131.8, 128.4, 127.0, 125.4, 124.4, 115.2, 20.2 ppm. HRMS (ESI): Calcd. for [M + H]$^+$ 332.1035, found 332.1067.

2-{5-[(6-Methyl-2-oxo-1,2-dihydroquinolin-3-yl)methylene]-4-oxo-2-thioxothiazolidin-3-yl}acetic Acid (MQR): Yield 84%. ^{1}H NMR (400 MHz, [D$_6$]DMSO): δ = 12.20 (s, 1 H), 8.34 (s, 1 H), 7.76 (s, 1 H), 7.58 (s, 1 H), 7.45 (d, J = 8.0 Hz, 1 H), 7.25 (d, J = 8.4 Hz, 1 H), 4.72 (s, 2 H), 2.35 (s, 3 H) ppm. ^{13}C NMR (100 MHz, [D$_6$]-DMSO): δ = 196.2, 167.3, 166.8, 160.3, 145.3, 137.5, 134.2, 131.9, 130.3, 128.5, 124.1, 123.4, 119.2, 115.2, 44.8, 20.2 ppm. HRMS (ESI): Calcd. for [M + H]$^+$ 361.0316; found 361.0370.

2-Cyano-3-(2-oxo-1,2-dihydrobenzo[*h*]quinolin-3-yl)acrylic Acid (BQC): Yield 80%. ^{1}H NMR (400 MHz, [D$_6$]DMSO): δ = 12.71 (s, 1 H), 8.94 (s, 2 H), 8.52 (s, 1 H), 8.03–8.01 (d, J = 7.6 Hz, 1 H), 7.73 (s, 3 H), 7.69 (s, 1 H) ppm. ^{13}C NMR (100 MHz, [D$_6$]DMSO): δ = 162.2, 148.8, 148.3, 147.3, 146.4, 138.8, 134.2, 130, 129.1, 128.9, 128.6, 128.2, 127.9, 126.9, 125.6, 124.9, 124.9, 124.5, 124.0, 123.2, 123.0, 114.9, 109.4, 104.1, 22.1 ppm. HRMS (ESI): Calcd. for [M + H]$^+$ 291.0769; found 291.0804.

2-(4-Nitrophenyl)-3-(2-oxo-1,2-dihydrobenzo[*h*]quinolin-3-yl)acrylonitrile (BQN): Yield 74%. ^{1}H NMR (400 MHz, [D$_6$]DMSO): δ = 9.06 (s, 1 H), 8.85 (s, 1 H), 8.22 (d, J = 8.8 Hz, 2 H), 8.04 (s, 1 H), 7.81–7.76 (m, 4 H), 7.65 (d, J = 9.2 Hz, 3 H) ppm. HRMS (ESI): Calcd. for [M + H]$^+$ 368.1035; found 368.1145.

2-{4-Oxo-5-[(2-oxo-1,2-dihydrobenzo[*h*]quinolin-3-yl)methylene]-2-thioxothiazolidin-3-yl}acetic Acid (BQR): Yield 70%. ^{1}H NMR (400 MHz, [D$_6$]DMSO): δ = 12.67 (s, 1 H), 8.89 (d, J = 8 Hz, 1 H), 8.51 (s, 1 H), 7.99 (d, J = 8 Hz, 1 H), 7.80 (s, 1 H), 7.75–7.65 (m, 4 H), 4.72 (s, 2 H) ppm. ^{13}C NMR (100 MHz, [D$_6$]DMSO): δ = 167.3, 166.8, 161.2, 134.2, 130.2, 129.2, 128.6, 127.0, 125.5, 123.3, 123.2, 122.8, 115.8, 44.9 ppm. HRMS (ESI): Calcd. for [M + H]$^+$ 397.0316; found 397.0410.

General Procedure for the Preparation of OMQA, NMQA and OBQA: MQA or BQA (1 equiv.) and K_2CO_3 (3 equiv.) were suspended in DMF and heated to 120 °C. At 120 °C, 1-bromooctane (1 equiv.) was added and the mixture was stirred at 120 °C until the reactant spot was no longer visible by TLC. Upon completion, the reaction mixture was cooled to room temperature and poured into demineralised water and extracted with chloroform. The crude product was purified by column chromatography. For BQA, one spot was visible by TLC and column chromatography (hexane/ethyl acetate, 1:0.03) gave the pure product. For MQA, hexane/ethyl acetate (1:0.02) was used as eluent to obtain the first spot, and the second spot was separated in hexane/ethyl acetate (1:0.06).

6-Methyl-2-(octyloxy)quinoline-3-carbaldehyde (OMQA): Yield 27%. ^{1}H NMR (400 MHz, [D$_6$]DMSO): δ = 10.49 (s, 1 H), 8.5 (s, 1 H), 7.73 (d, J = 8.4 Hz, 1 H), 7.54–7.59 (m, 2 H), 4.56 (t, J = 6.8 Hz, 2 H), 2.49 (s, 3 H), 1.84–1.91 (m, 2 H), 1.47–1.54 (m, 3 H), 1.28–1.41 (m, 7 H), 0.89 (t, J = 6.8 Hz, 3 H) ppm. ^{13}C NMR (100 MHz, [D$_6$]DMSO): δ = 189.6, 160.8, 147.5, 138.9, 134.6, 134.5, 128.6, 126.9, 124.2, 119.9, 66.5, 31.8, 29.7, 29.3, 29.2, 28.9, 26.2, 22.6, 21.2, 14.1 ppm. MS (ESI): Calcd. for [M + H]$^+$ 300.2; found 300.25.

2-(Octyloxy)benzo[*h*]quinoline-3-carbaldehyde (OBQA): Yield 87%. ^{1}H NMR (400 MHz, [D$_6$]DMSO): δ = 10.55 (s, 1 H), 9.12–9.14 (m, 1 H), 8.6 (s, 1 H), 7.87–7.89 (m, 1 H), 7.68–7.74 (m, 4 H), 4.74 (t, J = 6.8 Hz, 2 H), 1.92–1.99 (m, 2 H), 1.31–1.46 (m, 10 H), 0.89 (t, J = 6.8 Hz, 3 H) ppm. ^{13}C NMR (100 MHz, [D$_6$]DMSO): δ = 189.3, 161.5, 148.1, 138.5, 135.0, 130.2, 129.2, 127.8, 126.7, 125.7, 125.7, 125.3, 121.4, 119.0, 127.8, 126.7, 125.7, 125.7, 125.3, 121.4, 119.0,66.7, 31.8, 29.4, 29.3, 28.9, 26.2, 22.7, 14.1 ppm. MS (ESI): Calcd. for [M + H]$^+$ 336.2; found 336.17.

6-Methyl-1-octyl-2-oxo-1,2-dihydroquinoline-3-carbaldehyde (NMQA): Yield 22%. ^{1}H NMR (400 MHz, [D$_6$]DMSO): δ = 10.48 (s, 1 H), 8.3 (s, 1 H), 7.51 (d, J = 6.8 Hz, 2 H), 7.29 (d, J = 9.6 Hz, 1 H), 4.29 (t, J = 8.0 Hz, 2 H), 2.43 (s, 3 H), 1.76 (m, 2 H), 1.44–1.61 (m, 3 H), 1.28–1.39 (m, 7 H), 0.88 (t, J = 6.8 Hz, 3 H) ppm. ^{13}C NMR (100 MHz, [D$_6$]DMSO): δ = 190.5, 161.5, 140.7, 139.5, 135.2, 132.4, 131.5, 125.1, 119.5, 114.4, 42.4, 31.7, 29.3, 29.2, 27.5, 27.0, 22.6, 20.4, 14.0 ppm. MS (ESI): Calcd. for [M + H]$^+$ 300.2; found 300.25.

General Procedure for the Preparation of NMQX, OMQX and OBQX (X = C, R) Compounds: To a mixture of alkylated quinolinone aldehyde (NMQA or OMQA or OBQA; 1 equiv.) and corresponding active methylene compound (1 equiv.) in chloroform, piperidine (0.01 equiv.) was added and the mixture was heated to reflux until the aldehyde spot was no longer visible by TLC. Upon

completion of the reaction, the precipitated solid was filtered and dried in vacuo to give the desired product.

General Procedure for the Preparation of NMQN, OMQN and OBQN Compounds: To a mixture of alkylated quinolinone aldehyde (NMQA or OMQA or OBQA; 1 equiv.) and corresponding active methylene compound (1 equiv.) in acetonitrile, piperidine (0.01 mol ratio) was added and the mixture was heated to reflux until the aldehyde spot was no longer visible by TLC. Upon completion of the reaction, the precipitated solid was filtered and dried in vacuo to yield the desired product.

2-Cyano-3-(6-methyl-1-octyl-2-oxo-1,2-dihydroquinolin-3-yl)acrylic Acid (NMQC): Yield 48%. ^{1}H NMR (400 MHz, $CDCl_3$): δ = 8.87 (d, J = 6.4 Hz, 2 H), 7.54 (s, 1 H), 7.51 (dd, J = 8.8, 1.6 Hz, 1 H), 7.28 (d, J = 4.4 Hz, 1 H), 4.3 (t, J = 8 Hz, 2 H), 2.43 (s, 3 H), 1.78–1.73 (q, J = 7.6 Hz, 2 H), 1.46–1.25 (m, 10 H), 0.88 (t, J = 6.8 Hz, 3 H) ppm. ^{13}C NMR (100 MHz, [D_6]DMSO): δ = 162.8, 159.3, 148.3, 140.1, 138.0, 134.9, 132.0, 130.2, 122.6, 118.9, 115.6, 114.8, 105.3, 42.2, 31.1, 28.6, 28.5, 26.9, 26.1, 22.0, 19.8, 13.8 ppm. HRMS (ESI): Calcd. for [M + H]$^+$ 367.2021; found 367.2243.

3-(6-Methyl-1-octyl-2-oxo-1,2-dihydroquinolin-3-yl)-2-(4-nitrophenyl)acrylonitrile (NMQN): Yield 59%. ^{1}H NMR (400 MHz, [D_6]-DMSO): δ = 8.77 (s, 1 H), 8.32–8.29 (m, 3 H), 7.9 (dd, J = 7.2, 1.6 Hz, 2 H), 7.54 (s, 1 H), 7.48 (dd, J = 8.8, 2 Hz, 1 H), 7.29 (d, J = 7.29 Hz, 1 H), 4.31 (t, J = 7.6 Hz, 2 H), 2.45 (s, 3 H), 1.76 (t, J = 8.0 Hz, 2 H), 1.57–1.27 (m, 10 H), 0.88 (t, J = 7.2 Hz, 3 H) ppm. ^{13}C NMR (100 MHz, $CDCl_3$): δ = 160.7, 147.9, 140.1, 139.7, 138.4, 137.8, 134.1, 132.5, 130.4, 126.8, 124.5, 124.3, 120.0, 117.0, 114.2, 110.3, 43.3, 31.7, 29.3, 29.1, 27.5, 27.0, 22.6, 20.4, 14.0 ppm. HRMS (ESI): Calcd. for [M + H]$^+$ 444.2287; found 444.2551.

2-{5-[(6-Methyl-1-octyl-2-oxo-1,2-dihydroquinolin-3-yl)methylene]-4-oxo-2-ioxothiazolidin-3-yl}acetic Acid (NMQR): Yield 69%. ^{1}H NMR (400 MHz, $CDCl_3$): δ = 7.9 (s, 1 H), 7.82 (s, 1 H), 7.45 (d, J = 5.2 Hz, 2 H), 7.24 (s, 1 H), 4.9 (s, 2 H), 4.27 (t, J = 8.0 Hz, 2 H), 2.43 (s, 3 H), 1.73 (t, J = 7.6 Hz, 2 H), 1.47–1.25 (m, 10 H), 0.88 (t, J = 6.8 Hz, 3 H) ppm. ^{13}C NMR (100 MHz, [D_6]DMSO): δ = 196.0, 167.2, 166.7, 159.4, 144.1, 137.3, 134.4, 132.0, 130.3, 129.8, 123.5, 123.2, 120.0, 114.7, 44.9, 43.6, 42.0, 31.1, 28.6, 28.5, 26.9, 26.2, 22.1, 22.0, 19.9, 13.8 ppm. HRMS (ESI): Calcd. for [M + H]$^+$ 473.1568; found 473.1874.

(*E*)-2-Cyano-3-[6-methyl-2-(octyloxy)quinolin-3-yl]acrylic Acid (OMQC): Yield 70%, ^{1}H NMR (400 MHz, [D_6]DMSO): δ = 12.67 (s, 1 H), 8.9–8.88 (d, J = 8 Hz, 1 H), 8.51 (s, 1 H), 8–7.98 (d, J = 8 Hz, 1 H), 7.80 (s, 1 H), 7.75–7.65 (m, 4 H), 4.72 (s, 2 H) ppm. ^{13}C NMR (100 MHz, [D_6]DMSO): δ = 162.7, 160.1, 158.1, 146.2, 145.4, 138.2, 137.8, 134.4, 134.0, 128.6, 128.0, 127.7, 127.5, 126.3, 124.1, 123.8, 118.2, 116.8,116.2, 66.2, 31.1, 30.3, 28.6, 28.5, 28.1, 25.4, 22.0, 20.8, 20.6, 20.1 ppm. HRMS (ESI): Calcd. for [M + H]$^+$ 367.2021; found 367.2171.

3-[6-Methyl-2-(octyloxy)quinolin-3-yl]-2-(4-nitrophenyl)acrylonitrile (OMQN): Yield 65%. ^{1}H NMR (400 MHz, $CDCl_3$): δ = 8.86 (s, 1 H), 8.35–8.32 (m, 2 H), 8.13 (s, 1 H), 7.89–7.87 (m, 2 H), 7.72 (d, J = 8.4 Hz, 1 H), 7.62 (s, 1 H), 7.53 (dd, J = 8.8, 2.0 Hz, 1 H), 4.53 (t, J = 6.8 Hz, 2 H), 2.51 (s, 3 H), 1.90–1.83 (m, 2 H), 1.51–1.25 (m, 10 H), 0.87 (t, J = 6.8 Hz, 3 H) ppm. ^{13}C NMR (100 MHz, $CDCl_3$): δ = 158.7, 147.9, 145.9, 140.3, 139.3, 137.2, 134.6, 133.7, 128.9, 127.7, 126.8, 126.7, 124.3, 117.8, 117.0, 110.8, 66.8, 31.8, 29.3, 29.2, 28.8, 26.2, 22.6,21.2, 14.0 ppm. HRMS (ESI): Calcd. for [M + H]$^+$ 444.2286; found 444.2293.

2-(5-{[6-Methyl-2-(octyloxy)quinolin-3-yl]methylene}-4-oxo-2-thioxothiazolidin-3-yl)acetic Acid (OMQR): Yield 69%. ^{1}H NMR (400 MHz, $CDCl_3$): δ = 8.14 (s, 1 H), 7.99 (s, 1 H), 7.7 (d, J = 8 Hz, 1 H), 7.53–7.5 (m, 2 H), 4.94 (s, 2 H), 4.53 (t, J = 6.4 Hz, 2 H), 2.49 (s, 3 H), 1.88 (t, J = 7.2 Hz, 2 H), 1.29–1.25 (m, 10 H), 0.88 (t, J = 6.4 Hz, 3 H) ppm. ^{13}C NMR (100 MHz, [D_6]DMSO): δ = 193.3, 167.1, 166.2, 158.0, 144.6, 139.4, 134.3, 133.8, 127.8, 126.8, 126.2, 124.3, 124.1, 117.5,66.3, 45.1, 31.1, 28.6, 28.5, 25.5, 25.5, 22.0, 20.7, 13.8 ppm. HRMS (ESI): Calcd. for [M + H]$^+$ 473.1568; found 473.1874.

2-Cyano-3-[2-(octyloxy)benzo[*h*]quinolin-3-yl]acrylic Acid (OBQC): Yield 56%. ^{1}H NMR (400 MHz, $CDCl_3$): δ = 9.14 (s, 1 H), 9.08 (s, 1 H), 8.88 (s, 1 H), 7.88–7.82 (m, 1 H), 7.69 (s, 4 H), 4.69 (t, J = 6 Hz, 2 H), 1.95 (t, J = 7.2 Hz, 2 H), 1.54–1.25 (m, 10 H), 0.88 (t, J = 6.4 Hz, 3 H) ppm. ^{13}C NMR (100 MHz, $CDCl_3$): δ = 162.8, 158.7, 146.4, 145.6, 138.2, 134.3, 129.2, 129.2, 127.9, 126.8, 125.6, 125.2, 124.2, 120.9, 116.0, 115.6, 66.5, 31.1, 28.6, 28.6, 28.1, 25.4, 22.0, 13.8 ppm. HRMS (ESI): Calcd. for [M + H]$^+$ 403.2180; found 403.2021.

2-(4-Nitrophenyl)-3-[2-(octyloxy)benzo[*h*]quinolin-3-yl]acrylonitrile (OBQN): Yield 67%. ^{1}H NMR (400 MHz, $CDCl_3$): δ = 9.13–9.10 (m, 1 H), 9.03 (s, 1 H), 8.34 (d, J = 8.8 Hz, 2 H), 8.20 (s, 1 H), 7.91–7.89 (m, 3 H), 7.74 (s, 2 H), 7.71–7.69 (m, 2 H), 4.73 (t, J = 6.8 Hz, 2 H), 2.00–1.93 (m, 2 H), 1.46–1.30 (m, 10 H), 0.87 (t, J = 6.8 Hz, 3 H) ppm. ^{13}C NMR (100 MHz, $CDCl_3$): δ = 159.2, 147.8, 146.1, 140.2, 138.5, 137.1, 134.7, 130.2, 128.9, 127.8, 126.7, 126.5, 125.7, 125.3, 124.8, 124.3, 121.5, 117.1, 116.8, 110.2, 67.1, 31.8, 29.4, 29.3, 28.9, 26.3, 22.7, 14.1, 4.7 ppm. HRMS (ESI): Calcd. for [M + H]$^+$ 480.2286; found 480.2527.

2-(5-{[2-(Octyloxy)benzo[*h*]quinolin-3-yl]methylene}-4-oxo-2-thioxothiazolidin-3-yl)acetic Acid (OBQR): Yield 67%. ^{1}H NMR (400 MHz, $CDCl_3$): δ = 9.10 (t, J = 4.4 Hz, 1 H), 8.21 (s, 1 H), 8.12 (s, 1 H), 7.89–7.87 (m, 1 H), 7.73–7.67 (m, 4 H), 4.96 (s, 2 H), 4.73 (t, J = 6.8 Hz, 2 H), 2.01–1.94 (m, 2 H), 1.45–1.25 (m, 10 H), 0.88 (t, J = 6.8 Hz, 3 H) ppm. ^{13}C NMR (100 MHz, $CDCl_3$): δ = 193.1, 167.1, 166.1, 158.5, 144.5, 139.3, 134.2, 129.2, 128.9, 127.9, 126.7, 126.5, 125.4, 125.3, 124.1, 123.6, 121.5, 116.5, 66.5, 45.1, 31.1, 28.7, 28.6, 28.1, 25.5, 22.0, 13.8 ppm. HRMS (ESI): Calcd. for [M + H]$^+$ 509.1568; found 509.1844.

Theoretical Calculations: To understand the structure-property relationships in the synthesised quinolinone compounds, DFT calculations were performed. Gas-phase optimisation of these molecules were carried out at the B3LYP/6-31g(d) level. B3LYP[27] functional is found to perform well for most organic molecules, and therefore was adopted here.[28] All the optimised structures were confirmed by the vibrational frequency calculations by obtaining no imaginary frequencies. In an effort to rationalise the nature of electronic transitions, the contributing configurations to the transitions and charge transfer probability, the ten lowest singlet excited states were calculated by means of TDDFT at the B3LYP/6-31g(d) level in THF solvent by using the ground-state optimised geometries. The Polarisable Continuum Model (PCM) was used to examine solvent effects.[29] All the calculations were carried out with the Gaussian 09 suite of program.[30]

Supporting Information (see footnote on the first page of this article): ^{1}H and ^{13}C NMR spectra, solvatochromatic spectra and their data, DFT optimized geometries, Frontier Molecular Orbitals and results of percentage contribution towards FMOs.

Acknowledgments

R. R. thanks the Department of Science and Technology (DST) (reference number SR/S1/PC-12/2011, DT: 20.09.2011) for the pro-

ject. G. P. thanks the University Grants Commission (UGC) (reference number 07722/E15/2012, Dt: 28.03.2012) for a fellowship. S. J. thanks the UGC BSR (reference number 039680/E15/ 2011, Dt: 17.02.2011) for a fellowship. R. V. S. thanks the UGC for financial support through the Maulana Azad National Fellowship [reference number F.40-17(C/M)/2009(SA-III/MANF)]. P. V. thanks the UGC for Emeritus Fellowship [F.6-6/2012-2013/EMERITUS-2012-2013-GEN-1171/(SA-II)]. The authors also thank UGC/DST-FIST for instrumental facilities in the School of Chemistry, Bharathidasan University, and the Sophisticated Analytical Instrument facility (SAIF), Indian Institute of Technology Madras (IIT Madras), for providing single-crystal X-ray analysis. The authors thank the reviewers for their helpful and suggestive comments.

[1] a) N. S. S. Kumar, M. D. Gujrati, J. N. Wilson, *Chem. Commun.* **2010**, *46*, 5464–5466; b) R. Menzel, S. Kupfer, R. Mede, D. Weiß, H. Görls, L. González, R. Beckert, *Eur. J. Org. Chem.* **2012**, 5231–5247; c) X. Y. Lauteslager, I. H. M. van Stokkum, H. J. van Ramesdonk, D. Bebelaar, J. Fraanje, K. Goubitz, H. Schenk, A. M. Brouwer, J. W. Verhoeven, *Eur. J. Org. Chem.* **2001**, 3105–3118; d) C. A. van Walree, V. E. M. Kaats-Richters, S. J. Veen, B. Wieczorek, J. H. van der Wiel, B. C. van der Wiel, *Eur. J. Org. Chem.* **2004**, 3046–3056; e) H. K. Shim, C. B. Yoon, T. Ahn, D. H. Hwang, T. Zyung, *Synth. Met.* **1999**, *101*, 134–135; f) S. W. Thomas, G. D. Joly, T. M. Swager, *Chem. Rev.* **2007**, *107*, 1339–1386; g) C. T. Chen, *Chem. Mater.* **2004**, *16*, 4389–4400; h) N. Martínez de Baroja, J. Garín, J. Orduna, R. Andreu, M. J. Blesa, B. Villacampa, R. Alicante, S. Franco, *J. Org. Chem.* **2012**, *77*, 4634–4644; i) N. Dash, G. Krishnamoorthy, *Photochem. Photobiol. Sci.* **2011**, *10*, 939–946; j) J. Chen, W. Liu, J. Ma, H. Xu, J. Wu, X. Tang, Z. Fan, P. Wang, *J. Org. Chem.* **2012**, *77*, 3475–3482; k) P. Heremans, D. Cheyns, B. P. Rand, *Acc. Chem. Res.* **2009**, *42*, 1740–1747; l) N. Martín, L. Sánchez, M. Á. Herranz, B. Illescas, D. M. Guldi, *Acc. Chem. Res.* **2007**, *40*, 1015–1024; m) T. Michinobu, C. Boudon, J.-P. Gisselbrecht, P. Seiler, B. Frank, N. N. P. Moonen, M. Gross, F. Diederich, *Chem. Eur. J.* **2006**, *12*, 1889–1905; n) A. A. Vasilev, K. De Mey, I. Asselberghs, K. Clays, B. Champagne, S. E. Angelova, M. I. Spassova, C. Li, K. Müllen, *J. Phys. Chem. C* **2012**, *116*, 22711–22719.

[2] a) N. S. S. Kumar, M. D. Gujrati, J. N. Wilson, *Chem. Commun.* **2010**, *46*, 5464–5466; b) C. A. Sierra, P. M. Lahti, *J. Phys. Chem. A* **2006**, *110*, 12081–12088; c) M. Manoharan, K. L. Tivel, M. Zhao, K. Nafisi, T. L. Netzel, *J. Phys. Chem.* **1995**, *99*, 17461–17472; d) A. A. Vasilev, K. De Mey, I. Asselberghs, K. Clays, B. Champagne, S. E. Angelova, M. I. Spassova, C. Li, K. Müllen, *J. Phys. Chem. C* **2012**, *116*, 22711–22719; e) L. Xu, C. Liu, Z. Qin, R. Jiang, Y. Li, *Eur. J. Org. Chem.* **2013**, 300–306; f) Y. Liu, S. Xiao, H. Li, Y. Li, H. Liu, F. Lu, J. Zhuang, D. Zhu, *J. Phys. Chem. B* **2004**, *108*, 6256–6260; g) N. Prachumrak, S. Namuangruk, T. Keawin, S. Jungsuttingwong, T. Sudyoadsuk, V. Promarak, *Eur. J. Org. Chem.* **2013**, 3825–3834; h) T. Sudyoadsuk, S. Pansay, S. Morada, R. Rattanawan, S. Namuangruk, T. Kaewin, S. Jungsuttiwong, V. Promarak, *Eur. J. Org. Chem.* **2013**, 5051; i) X. Zhang, Y. Wu, S. Ji, H. Guo, P. Song, K. Han, W. Wu, T. D. James, J. Zhao, *J. Org. Chem.* **2010**, *75*, 2578–2588; j) J. Chen, W. Liu, J. Ma, H. Xu, J. Wu, X. Tang, Z. Fan, P. Wang, *J. Org. Chem.* **2012**, *77*, 3475–3482; k) Z. S. Wang, Y. Cui, Y. Dan-oh, C. Kasada, A. Shinpo, K. Hara, *J. Phys. Chem. C* **2007**, *111*, 7224–7230; l) A. P. Kulkarni, P. T. Wu, T. W. Kwon, S. A. Jenekhe, *J. Phys. Chem. B* **2005**, *109*, 19584–19594; m) M. Singh, R. Kurchania, J. A. Mikroyannidis, S. S. Sharma, G. D. Sharma, *J. Mater. Chem. A* **2013**, *1*, 2297–2306; n) J. Mao, N. He, Z. Ning, Q. Zhang, F. Guo, L. Chen, W. Wu, J. Hua, H. Tian, *Angew. Chem.* **2012**, *124*, 10011; *Angew. Chem. Int. Ed.* **2012**, *51*, 9873–9876; o) Y. Li, T. Ren, W. J. Dong, *J. Photochem. Photobiol. A: Chem.* **2013**, *251*, 1–9; p) X. Tang, W. Liu, J. Wu, C. Sing Lee, J. You, P. Wang, *J. Org. Chem.* **2010**, *75*, 7273–7278; q) S. Ito, S. M. Zakeeruddin, R. Humphry-Baker, P. Liska, R. Charvet, P. Comte, M. K. Nazeeruddin, P. Péchy, M. Takata, H. Miura, S. Uchida, M. Grätzel, *Adv. Mater.* **2006**, *18*, 1202–1205; r) H. Chen, H. Huang, X. Huang, J. N. Clifford, A. Forneli, E. Palomares, X. Zheng, L. Zheng, X. Wang, P. Shen, B. Zhao, S. Tan, *J. Phys. Chem. C* **2010**, *114*, 3280–3286; s) G. Paramaguru, R. Vijay Solomon, S. Jagadeeswari, P. Venuvanalingam, R. Renganathan, *J. Photochem. Photobiol. A: Chem.* **2013**, *271*, 31–44.

[3] a) S. Park, J. E. Kwon, S. H. Kim, J. Seo, K. Chung, S. Y. Park, D. J. Jang, B. M. Medina, J. Gierschner, S. Y. Park, *J. Am. Chem. Soc.* **2009**, *131*, 14043–14049; b) J. Shao, S. Ji, X. Li, J. Zhao, F. Zhou, H. Guo, *Eur. J. Org. Chem.* **2011**, 6100–6109; c) L. Chen, T. S. Hu, Z. J. Yao, *Eur. J. Org. Chem.* **2008**, 6175–6182; d) L. Giordano, V. V. Shvadchak, J. A. Fauerbach, E. A. Jares-Erijman, T. M. Jovin, *J. Phys. Chem. Lett.* **2012**, *3*, 1011–1016; e) L. Xie, Y. Chen, W. Wu, H. Guo, J. Zhao, X. Yu, *Dyes Pigm.* **2012**, *92*, 1361–1369; f) J. Catalán, J. C. del Valle, R. M. Claramunt, D. Sanz, J. Dotor, *J. Lumin.* **1996**, *68*, 165–170; g) A. Sytnik, M. Kasha, *Proc. Natl. Acad. Sci. USA* **1994**, *91*, 8627–8630; h) K. I. Sakai, T. Tsuzuki, Y. Itoh, M. Ichikawa, Y. Taniguchi, *Appl. Phys. Lett.* **2005**, *86*, 081103.

[4] a) M. Komatsu, J. Nakazaki, S. Uchida, T. Kubo, H. Segawa, *Phys. Chem. Chem. Phys.* **2013**, *15*, 3227–3232; b) M. Komatsu, J. Nakazaki, S. Uchida, T. Kubo, H. Segawa, *Phys. Chem. Chem. Phys.* **2013**, *15*, 3227–3232; c) D. Huang, Y. Chen, J. Zhao, *Dyes Pigm.* **2012**, *95*, 732–742; d) Y. Li, T. Ren, W. J. Dong, *J. Photochem. Photobiol. A: Chem.* **2013**, *251*, 1–9.

[5] a) J. Piechowska, D. T. Gryko, *J. Org. Chem.* **2011**, *76*, 10220–10228; b) S. Kim, J. Seo, H. K. Jung, J. J. Kim, S. Y. Park, *Adv. Mater.* **2005**, *17*, 2077–2082.

[6] a) M. R. Nimlos, D. F. Kelley, E. R. Bernstein, *J. Phys. Chem.* **1987**, *91*, 6610–6614; b) A. Held, D. F. Plusquellic, J. L. Tomer, D. W. Pratt, *J. Phys. Chem.* **1991**, *95*, 2877–2881; c) A. Gerega, L. Lapinski, M. J. Nowak, A. Furmanchuk, J. Leszczynski, *J. Phys. Chem. A* **2007**, *111*, 4934–4943; d) V. Arun, S. Mathew, P. P. Robinson, M. Jose, V. P. N. Nampoori, K. K. M. Yusuff, *Dyes Pigm.* **2010**, *87*, 149–157; e) C. Charitos, C. Tzougraki, G. Kokotos, *J. Pept. Res.* **2000**, *56*, 373–381.

[7] a) X. Chen, K. Kobiro, H. Asahara, K. Kakiuchi, R. Sugimoto, K. Saigo, N. Nishiwaki, *Tetrahedron* **2013**, *69*, 4624–4630; b) N. Nishiwaki, R. Sugimoto, K. Saigo, K. Kobiro, *Tetrahedron Lett.* **2013**, *54*, 956–959; c) M. Asahara, M. Ohtsutsumi, M. Ariga, N. Nishiwaki, *Heterocycles* **2009**, *78*, 2851–2854; d) M. Asahara, T. Katayama, Y. Tohda, N. Nishiwaki, M. Ariga, *Chem. Pharm. Bull.* **2004**, *52*, 1334–1338.

[8] a) D. Senthil Raja, E. Ramachandran, N. S. P. Bhuvanesh, K. Natarajan, *Eur. J. Med. Chem.* **2013**, *64*, 148–159; b) D. Senthil Raja, G. Paramaguru, N. S. P. Bhuvanesh, J. H. Reibenspies, R. Renganathan, K. Natarajan, *Dalton Trans.* **2011**, *40*, 4548–4559; c) E. Ramachandran, D. Senthil Raja, N. P. Rath, K. Natarajan, *Inorg. Chem.* **2013**, *52*, 1504–1514.

[9] a) S. L. Suraru, U. Zschieschang, H. Klauk, F. Wurthner, *Chem. Commun.* **2011**, *47*, 1767–176; b) M. A. Naik, N. Venkatramaiah, C. Kanimozhi, S. Patil, *J. Phys. Chem. C* **2012**, *116*, 26128–26137; c) E. Zhou, S. Yamakawa, K. Tajima, C. Yang, K. Hashimoto, *Chem. Mater.* **2009**, *21*, 4055–4061; d) P. E. Hansen, F. Duus, S. Bolvig, T. S. Jagodzinski, *J. Mol. Struct.* **1996**, *378*, 45–59.

[10] a) T. Beyerlein, B. Tieke, *Macromol. Rapid Commun.* **2000**, *21*, 182–189; b) A. B. Tamayo, M. Tantiwiwat, B. Walker, T.-Q. Nguyen, *J. Phys. Chem. C* **2008**, *112*, 15543–15552; c) S. J. Evenson, T. M. Pappenfus, M. C. R. Delgado, K. R. Radke-Wohlers, J. T. L. Navarrete, S. C. Rasmussen, *Phys. Chem. Chem. Phys.* **2012**, *14*, 6101–6111.

[11] a) B. Baruah, P. J. Bhuyan, *Tetrahedron* **2009**, *65*, 7099–7104.

[12] a) R. Y. Lin, C. Lee, Y. Chen, J. Peng, T. C. Chou, H. Yang, J. T. Lina, K. Ho, *Chem. Commun.* **2012**, *48*, 12071–12073; b) B. Zhang, J. Sun, C. Bi, G. Yin, L. Pu, Y. Shi, L. Sheng, *New J. Chem.* **2011**, *35*, 849–853.

[13] a) S. Ferrer, D. P. Naughton, I. Parveen, M. D. Threadgill, *J. Chem. Soc. Perkin Trans. 1* **2002**, 335–340; b) F. H. Greenberg, *J. Chem. Educ.* **1990**, *67*, 611; c) Z. X. Guo, A. N. Cammidge, A. McKillop, D. C. Horwell, *Tetrahedron Lett.* **1999**, *40*, 6999–7002; d) S. Frebort, Z. Eliáš, A. Lyčka, S. Luňák Jr., J. Vyňuchal, L. Kubáč, R. Hrdina, L. Burgert, *Tetrahedron Lett.* **2011**, *52*, 5769–5773; e) E. L. Lanni, M. A. Bosscher, B. D. Ooms, C. A. Shandro, B. A. Ellsworth, C. E. Anderson, *J. Org. Chem.* **2008**, *73*, 6425–6428; f) D. Conreaux, E. Bossharth, N. Monteiro, P. Desbordes, G. Balme, *Tetrahedron Lett.* **2005**, *46*, 7917–7920; g) H. Liu, S. B. Ko, H. Josien, D. P. Curran, *Tetrahedron Lett.* **1995**, *36*, 8917–8920; h) X. Yu, S. Eymur, V. Singh, B. Yang, M. Tonga, A. Bheemaraju, G. Cooke, C. Subramani, D. Venkataraman, R. J. Stanley, V. M. Rotello, *Phys. Chem. Chem. Phys.* **2012**, *14*, 6749–6754; i) M. S. Shmidt, A. M. Reverdito, L. Kremenchuzky, I. A. Perillo, M. M. Blanco, *Molecules* **2008**, *13*, 831–840; j) M. Navid Soltani Rad, A. Khalafi-Nezhad, S. Babamohammadi, S. Behrouz, *Helv. Chim. Acta* **2010**, *93*, 2454–2466; k) T. C. Ko, M. J. Hour, J. C. Lien, C. M. Teng, K. H. Lee, S. C. Kuo, L. J. Huang, *Bioorg. Med. Chem. Lett.* **2001**, *11*, 279–282; l) M. Hadjeri, A. M. Mariotte, A. Boumendjel, *Chem. Pharm. Bull.* **2001**, *49*, 1352–1355; m) M. C. Torhan, N. P. Peet, J. D. Williams, *Tetrahedron Lett.* **2013**, *54*, 3926–3928.

[14] CCDC-951356 (for OBQA) contains the supplementary crystallographic data for this paper. These data can be obtained free of charge from The Cambridge Crystallographic Data Centre via www.ccdc.cam.ac.uk/data_request/cif.

[15] a) A. Baheti, C. H. Lee, K. R. J. Thomas, K. C. Ho, *Phys. Chem. Chem. Phys.* **2011**, *13*, 17210–17221.

[16] a) W. Xu, B. Peng, J. Chen, M. Liang, F. Cai, *J. Phys. Chem. C* **2008**, *112*, 874–880; b) S. Roquet, A. Cravino, P. Leriche, O. Alévéque, P. Frére, J. Roncali, *J. Am. Chem. Soc.* **2006**, *128*, 3459–3466; c) A. P. Kulkarni, P. T. Wu, T. W. Kwon, S. A. Jenekhe, *J. Phys. Chem. B* **2005**, *109*, 19584–19594.

[17] a) K. R. J. Thomas, N. Kapoor, M. N. K. P. Bolisetty, J. H. Jou, Y. L. Chen, Y. C. Jou, *J. Org. Chem.* **2012**, *77*, 3921–3932; b) P. Singh, A. Baheti, K. R. J. Thomas, *J. Org. Chem.* **2011**, *76*, 6134–6145; c) Q. Feng, Q. Zhang, X. Lu, H. Wang, G. Zhou, Z. Wang, *ACS Appl. Mater. Interfaces* **2013**, *5*, 8982–8990; d) D. Huang, Y. Chen, J. Zhao, *Dyes Pigm.* **2012**, *95*, 732–742.

[18] N. Nishiwaki, *Molecules* **2010**, *15*, 5174–5195.

[19] K. R. J. Thomas, N. Kapoor, M. N. K. P. Bolisetty, J. H. Jou, Y. L. Chen, Y. C. Jou, *J. Org. Chem.* **2012**, *77*, 3921–3932.

[20] R. Lartia, C. Allain, G. Bordeau, F. Schmidt, C. F-Debuisschert, F. Charra, M. Teulade-Fichou, *J. Org. Chem.* **2008**, *73*, 1732–1744.

[21] W. Zhang, W. Mao, Y. Hu, Z. Tian, Z. Wang, Q. Meng, *J. Phys. Chem. A* **2009**, *113*, 9997–10004.

[22] a) S. Erten-Ela, S. Ozcelik, E. Eren, *J. Fluoresc.* **2011**, *21*, 1565–1573; b) M. Takara, A. S. Ito, *J. Fluoresc.* **2005**, *15*, 171–177; c) K. Panthi, R. M. Adhikari, T. H. Kinstle, *J. Phys. Chem. A* **2010**, *114*, 4550–4557; d) A. Filarowski, M. Kluba, K. Cieślik-Boczula, A. Koll, A. Kochel, L. Pandey, W. M. D. Borggraeve, M. V. D. Auweraer, J. Catalán, N. Boens, *Photochem. Photobiol. Sci.* **2010**, *9*, 996–1008; e) J. Catalán, *J. Phys. Chem. B* **2009**, *113*, 5951–5960.

[23] a) A. Baheti, C. H. Lee, K. R. J. Thomas, K. C. Ho, *Phys. Chem. Chem. Phys.* **2011**, *13*, 17210–17221; b) L. Alibabaei, J. H. Kim, M. Wang, N. Pootrakulchote, J. Teuscher, D. Di Censo, R. Humphry-Baker, J. E. Moser, Y. J. Yu, K. Y. Kay, S. M. Zakeeruddin, M. Grtzel, *Energy Environ. Sci.* **2010**, *3*, 1757–1764; c) S. H. Kim, H. W. Kim, C. Sakong, J. Namgoong, S. W. Park, M. J. Ko, C. H. Lee, W. I. Lee, J. P. Kim, *Org. Lett.* **2011**, *13*, 5784–5787; d) D. Cao, J. Peng, Y. Hong, X. Fang, L. Wang, H. Meier, *Org. Lett.* **2011**, *13*, 1610–1613; e) K. Srinivas, K. Yesudas, K. Bhanuprakash, V. J. Rao, L. Giribabu, *J. Phys. Chem. C* **2009**, *113*, 20117–20126.

[24] S. Achelle, F. Guen, *Tetrahedron Lett.* **2013**, *54*, 4491–4496.

[25] a) M. K. Nazeeruddin, M. Amirnasr, P. Comte, J. R. Mackay, A. J. McQuillan, R. Houriet, M. Grtzel, *Langmuir* **2000**, *16*, 8525–8528.

[26] a) A. L. Tenderholt, *QMForge*, version 2.1, Stanford University, Stanford, CA, **2007**; b) A. L. Q. Tenderholt, version 2.1, http://qmforge.sourceforge.net.

[27] a) A. D. Becke, *J. Chem. Phys.* **1993**, *98*, 5648–5652; b) C. Lee, W. Yang, R. G. Parr, *Phys. Rev. B* **1988**, *37*, 785–789.

[28] a) L. A. Curtiss, K. Raghavachari, P. C. Redfern, J. A. Pople, *Chem. Phys. Lett.* **1997**, *270*, 419–426; b) E. Kleinpeter, B. A. Stamboliyska, *J. Org. Chem.* **2008**, *73*, 8250–8255; c) R. V. Solomon, P. Veerapandian, S. A. Vedha, P. Venuvanalingam, *J. Phys. Chem. A* **2012**, *116*, 4667–4677.

[29] S. Miertus, E. Scrocco, J. Tomasi, *Chem. Phys.* **1981**, *55*, 117–129.

[30] M. J. Frisch, G. W. Trucks, H. B. Schlegel, G. E. Scuseria, M. A. Robb, J. R. Cheeseman, G. Scalmani, V. Barone, B. Mennucci, G. A. Petersson, H. Nakatsuji, M. Caricato, X. Li, H. P. Hratchian, A. F. Izmaylov, J. Bloino, G. Zheng, J. L. Sonnenberg, M. Hada, M. Ehara, K. Toyota, R. Fukuda, J. Hasegawa, M. Ishida, T. Nakajima, Y. Honda, O. Kitao, H. Nakai, T. Vreven Jr, J. A. Montgomery, J. E. Peralta, F. Ogliaro, M. Bearpark, J. J. Heyd, E. Brothers, K. N. Kudin, V. N. Staroverov, R. Kobayashi, J. Normand, K. Raghavachari, A. Rendell, J. C. Burant, S. S. Iyengar, J. Tomasi, M. Cossi, N. Rega, N. J. Millam, M. Klene, J. E. Knox, J. B. Cross, V. Bakken, C. Adamo, J. Jaramillo, R. Gomperts, R. E. Stratmann, O. Yazyev, A. J. Austin, R. Cammi, C. Pomelli, J. W. Ochterski, R. L. Martin, K. Morokuma, V. G. Zakrzewski, G. A. Voth, P. Salvador, J. J. Dannenberg, S. Dapprich, A. D. Daniels, Ö. Farkas, J. B. Foresman, J. V. Ortiz, J. Cioslowski, D. J. Fox, *Gaussian 09*, revision B.01, Gaussian, Inc., Wallingford CT, **2009**.

Received: July 21, 2013
Published Online: December 3, 2013

